



# Direct combination of hydrogen evolution from water and methane conversion in a photocatalytic system over Pt/TiO<sub>2</sub>

Linhui Yu, Yu Shao, Danzhen Li\*

State Key Laboratory of Photocatalysis on Energy and Environment, Research Institute of Photocatalysis, Fuzhou University, Fuzhou 350002, PR China

## ARTICLE INFO

### Article history:

Received 9 September 2016

Received in revised form

12 November 2016

Accepted 19 November 2016

Available online 20 November 2016

### Keywords:

Photocatalysis

CH<sub>4</sub> conversion

H<sub>2</sub> production

Photocatalytic efficiency

Synergy

## ABSTRACT

The CH<sub>4</sub> conversion under ambient condition remains a challenge over the past years, and the production of the ideal clean energy of H<sub>2</sub> is considered as an alternative method to meet the requirement of sustainable development. Herein, a new photocatalytic reaction system involved H<sub>2</sub> evolution from aqueous water and CH<sub>4</sub> conversion is established over Pt/TiO<sub>2</sub>. The synergistic effect between the two reactions of H<sub>2</sub> production and CH<sub>4</sub> conversion brings up the considerable quantum efficiencies of H<sub>2</sub> production to 4.7% without sacrificial agent and CH<sub>4</sub> conversion (the main products are C<sub>2</sub>H<sub>6</sub> and CO<sub>2</sub>) to 3.3% simultaneously. The introduction of Pt on the surface of TiO<sub>2</sub> particles facilitates the activation of CH<sub>4</sub> and •OH that can assist to produce methyl radical (•CH<sub>3</sub>), afterwards more C<sub>2</sub>H<sub>6</sub> (61.7% selectivity) is formed.

© 2016 Elsevier B.V. All rights reserved.

## 1. Introduction

Methane (CH<sub>4</sub>), occupying the primary component of natural gas, is nearly ubiquitous in the world. As a fuel, the commercial use of CH<sub>4</sub> by directly burning will result in much worse global warming than CO<sub>2</sub> [1,2]. Recent, the conversion of CH<sub>4</sub> to other high value-added products has received increasing attention because of their sustainability for energy and environment [3–14]. These processes often demand the high pressure or high temperature reaction conditions. Photocatalysis technology is recognized as an alternative solution to meet the green conversion of CH<sub>4</sub>, since the solar energy is by far the largest exploitable resource [15]. Some important achievements, such as non-oxidative coupling of CH<sub>4</sub> to higher hydrocarbons (ethane, ethylene, propane, n- and i-butane) and H<sub>2</sub> [16–18], CH<sub>4</sub> reforming with CO<sub>2</sub> or H<sub>2</sub>O (gas) to syngas [19–23], partial oxidation of methane to methanol [24–30], and even to benzene [31] are developed in recent years. Among these works, the conversion of CH<sub>4</sub> to syngas and methanol are most studied in photocatalysis. For the desired product of alkanes, such as C<sub>2</sub>H<sub>6</sub>, the efficiency is still in a low level at present [28,29,32]. As a high-valued product, C<sub>2</sub>H<sub>6</sub> is an important industrial raw material to produce C<sub>2</sub>H<sub>4</sub>, halogenated ethane, and aromatic hydrocarbon

[33–39]. It is therefore necessary to find an effective strategy to improve the yield of C<sub>2</sub>H<sub>6</sub>.

The H<sub>2</sub> production from water has been a hot topic in photocatalysis, but the use of a sacrificial reagent is necessary [40–44], even in Pt/TiO<sub>2</sub> catalyst system. In addition, the improvement of efficiency via simultaneous utilization of photo-induced electron and hole for two different catalytic reactions is still a rarity. In this work, the two photocatalytic reactions of CH<sub>4</sub> conversion and water splitting into H<sub>2</sub> are introduced simultaneously in one system, and the high-valued products of H<sub>2</sub> and C<sub>2</sub>H<sub>6</sub> are gained, which has not been reported. Here the CH<sub>4</sub> is introduced as the sacrificial agent for hole as well as the useful reactant converted into other hydrocarbon. Through this way, the photo-induced electron and hole can be efficiently separated and adequately utilized, and a new strategy about the direct combination of H<sub>2</sub> evolution from water and CH<sub>4</sub> conversion with high efficiency photocatalytic performance is achieved successfully.

## 2. Experimental methods

### 2.1. Materials

The commercial P25 (Degussa) is used as TiO<sub>2</sub> precursor. H<sub>2</sub>PtCl<sub>6</sub> and CH<sub>3</sub>OH were purchased as A.R. grade chemicals from Sinopharm Chemical Reagent Co., Ltd., Shanghai, China. 5, 5-dimethyl-1-pyrroline-N-oxide (DMPO) was obtained from J&K Chemical Ltd. The CH<sub>4</sub> (with purity ≥ 99.999%) was supplied by

\* Corresponding author.

E-mail addresses: [dzli@fzu.edu.cn](mailto:dzli@fzu.edu.cn), [danzli@126.com](mailto:danzli@126.com) (D. Li).

Fuzhou Xinhang gases co., Ltd. All of the reagents are used without further purification.

## 2.2. Sample preparation

The commercial  $\text{TiO}_2$  was dispersed in  $\text{H}_2\text{PtCl}_6$  solution with different mass fraction of Pt ( $x\% = 0.1\%, 0.3\%, 0.5\%, 1\%, 1.5\%, 2\%$ ). In the presence of  $\text{CH}_3\text{OH}$ , the mixture was irradiated by UV light of 254 nm for 1 h to produce  $\text{Pt}/\text{TiO}_2$ . Then resultant precipitate were harvested by centrifugation, then, washed with deionized water and absolute ethyl alcohol for several times. Finally, the obtained precipitate was dried at  $80^\circ\text{C}$  in oven.

## 2.3. Characterizations

X-ray diffraction (XRD) patterns were recorded on a Bruker D8 Advance X-ray diffractometer with  $\text{Cu K}\alpha$  radiation. The diffuse reflectance spectra (DRS) were performed on Varian Cary 500 UV-vis spectrophotometer with  $\text{BaSO}_4$  as the background ranging from 250 nm to 800 nm. The morphologies of the obtained products were observed by a transmission electron microscopy (TEM) (FEI Tecnai G2 F20 S-TWIN, operated at an accelerating voltage of 200 kV). X-ray photoelectron spectroscopy (XPS) analysis was collected on an ESCALAB 250 photoelectron spectrometer (Thermo Fisher Scientific) with monochromatic Al  $\text{K}\alpha$  radiation ( $E = 1486.2 \text{ eV}$ ). Electron spin resonance (ESR) spectra were obtained using a Bruker model A300 spectrometer with a Philip lamp of 254 nm as light source, and 5,5-dimethyl-l-pyrroline-N-oxide (DMPO) as trapper. All the samples are measured in suspension dispersed in various solutions. The sample is dispersed in purified methanol for detection of  $\cdot\text{O}_2^-$ , in deionized water for detection of  $\cdot\text{OH}$ , and in water dissolved  $\text{CH}_4$  for detection of  $\cdot\text{CH}_3$ .

## 2.4. Evaluation of photocatalytic properties

The photocatalytic activity of the catalyst was measured in a gas-liquid-solid system. 75 mg catalyst was dispersed in 75 mL  $\text{H}_2\text{O}$ , and the  $\text{CH}_4$  was filled upon the water with volume of 80 mL (including the gas circuit) at ordinary pressure. The reactant gas was circulated in the system with flow rate of 10 mL/min by a circulating pump. The reactant suspension was irradiated by UV lamps with a wavelength centered at 254 nm (Philips, TUV 4W/G4 T5). The reaction system was remained at  $25^\circ\text{C}$  by thermostatic water around. After irradiation for 6 h, the concentration of the gas sample was monitored from the reactor using a gas chromatograph Model HP 6890 (Agilent Technologies Inc., USA) equipped with TDX-01, thermal conductivity detector and flame ionization detector. The schematic of the experimental set up for this work is shown in Fig. S1.

## 3. Results and discussion

### 3.1. Morphology and optical properties of the samples

The XRD patterns of the samples with different fraction of Pt ( $x\%$ ) are displayed in Fig. 1. The crystal phase of anatase and rutile  $\text{TiO}_2$  in the samples is respectively marked as \* and ▲ according to the PDF no. 21-1272 and no. 21-1276 standard card. None of characteristic peaks belonging to Pt are observed due to its low proportion. And with the increasing of Pt proportion, a weak peak at  $39.8^\circ$  is detected, which can be indexed to the (111) plane of Pt (PDF no. 04-0802, labelled by ■). The intensity of  $\text{TiO}_2$  peaks decreases with the amount increasing of Pt. This may be attributed to the shelter of Pt on the surface of  $\text{TiO}_2$  particles, or the aggregation inhibition of  $\text{TiO}_2$  particles caused by the participation of Pt.

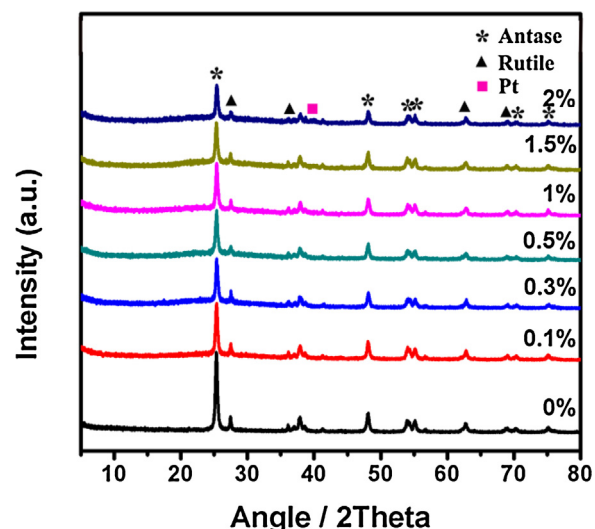


Fig. 1. The XRD patterns of the  $x\%$   $\text{Pt}/\text{TiO}_2$ .

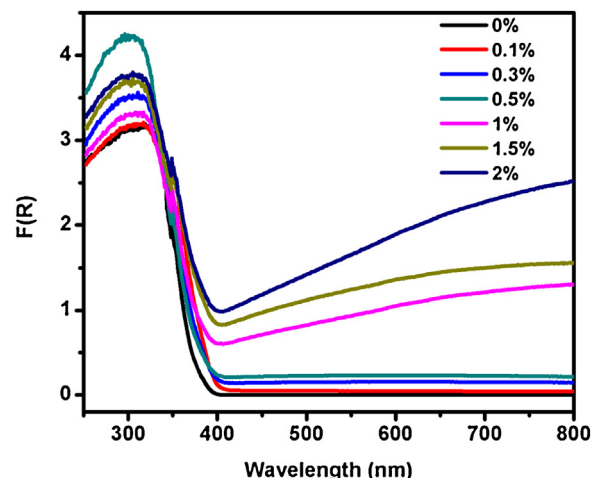
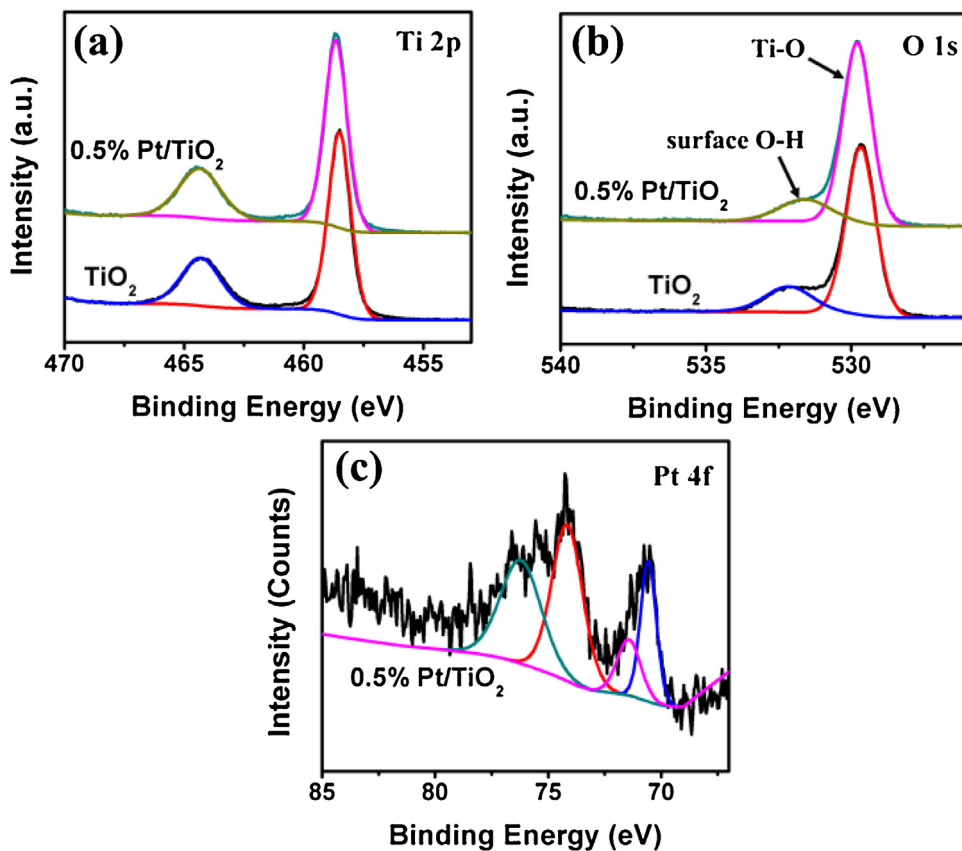


Fig. 2. The UV-vis diffuse reflectance spectra of the  $x\%$   $\text{Pt}/\text{TiO}_2$ .

The optical character of the samples was studied by using UV-vis diffuse reflectance spectra (see Fig. 2). It shows that  $\text{TiO}_2$  only absorbs the light in the UV region ( $\lambda < 400 \text{ nm}$ ), based on which the UV light is used as exciting light source. The introduction of the Pt increases the absorption in the visible light region, and the absorption is positive increased with the proportion of Pt. Besides, the introduction of Pt slightly shifts the absorption edge of the  $\text{TiO}_2$  to longer wavelength. The results indicate that the Pt is successfully loaded on the  $\text{TiO}_2$  particles.

XPS was carried out to further investigate the surface compositions and chemical states of 0.5%  $\text{Pt}/\text{TiO}_2$  and  $\text{TiO}_2$  (Fig. 3). From the results spectra of  $\text{Ti} 2\text{p}$  and  $\text{O} 1\text{s}$  of lattice oxygen at 529.8 eV, it shows peak-shifting to the higher binding energy, which can be the evidence for the interaction between Pt and  $\text{TiO}_2$ . The peak shifting to the lower binding energy of the oxygen of surface hydroxyl at 531.6 eV [45,46] indicates that Pt is interaction with surface oxygen. The fitted two pairs of Pt peaks are indexed to two states of Pt elements ( $\text{Pt}^0$ ,  $\text{Pt}^{2+}$ ).

The morphology nature of 0.5%  $\text{Pt}/\text{TiO}_2$  is characterized by transmission electron microscopy (TEM) in Fig. 4a. The dispersing Pt particles are smaller as compared to  $\text{TiO}_2$  particles. The identification of lattice fringes indicates the coexistence of anatase (A) and rutile (R)  $\text{TiO}_2$ , as shown in Fig. 4b. The particle with a deeper contrast of which the diameter is about 5 nm, obtains the lattice fringe



**Fig. 3.** XPS spectra of 0.5% Pt/TiO<sub>2</sub> and TiO<sub>2</sub>: (a) Ti 2p, (b) O 1s, (c) Pt 4f.

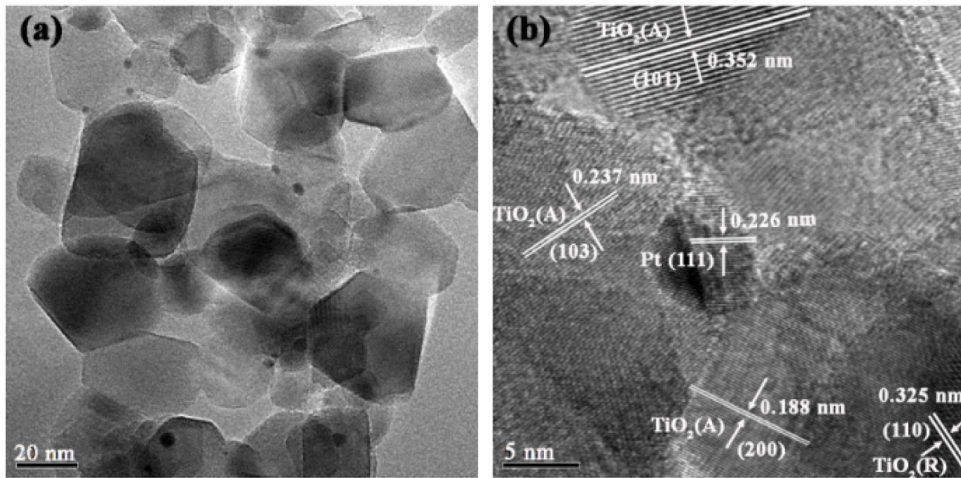


**Fig. 4.** The TEM (a) and high-resolution TEM (b) images of 0.5% Pt/TiO<sub>2</sub>.

indexed to the (111) crystallographic plane of Pt. Therefore, the sample of Pt supported on TiO<sub>2</sub> is successfully prepared.

### 3.2. Photocatalytic properties of the samples

The photocatalytic activities of x% Pt/TiO<sub>2</sub> are evaluated by the amount of H<sub>2</sub> production (Fig. 5a), the total conversion of CH<sub>4</sub> (Fig. 5b), as well as the distribution of carbonous gas products (Fig. 5c). Unlike the reported literatures on the conversion of CH<sub>4</sub> with liquid H<sub>2</sub>O [25,26,28,29,47–49], methanol is hardly detected in this system. It is found that the introduction of Pt obviously improves the amount of all the products. The H<sub>2</sub> production

increases with the increasing of Pt loading, and the maximum of 180 μmol is obtained at Pt fraction of 1.5% (see in Fig. 5a). More Pt (2%) does not result in a continuous increase of the H<sub>2</sub> production. While the total conversion of CH<sub>4</sub> increases with the increasing of Pt loading. The detailed distribution of the carbonous products changes with the increasing of C<sub>2</sub>H<sub>6</sub> and decreasing of CO<sub>2</sub> when Pt fraction varies from 0.1% to 0.5%. A little variation of C<sub>2</sub>H<sub>6</sub> and increasing of CO<sub>2</sub> can be found with Pt fraction varying from 1% to 2%. All the catalysts obtain little C<sub>2</sub>H<sub>6</sub> except 0.5% Pt/TiO<sub>2</sub>. And the product of CO over each photocatalyst remains almost constant, which indicates that CO may be the intermediate product for CO<sub>2</sub>. Additionally, we can conclude that the participation of Pt changes

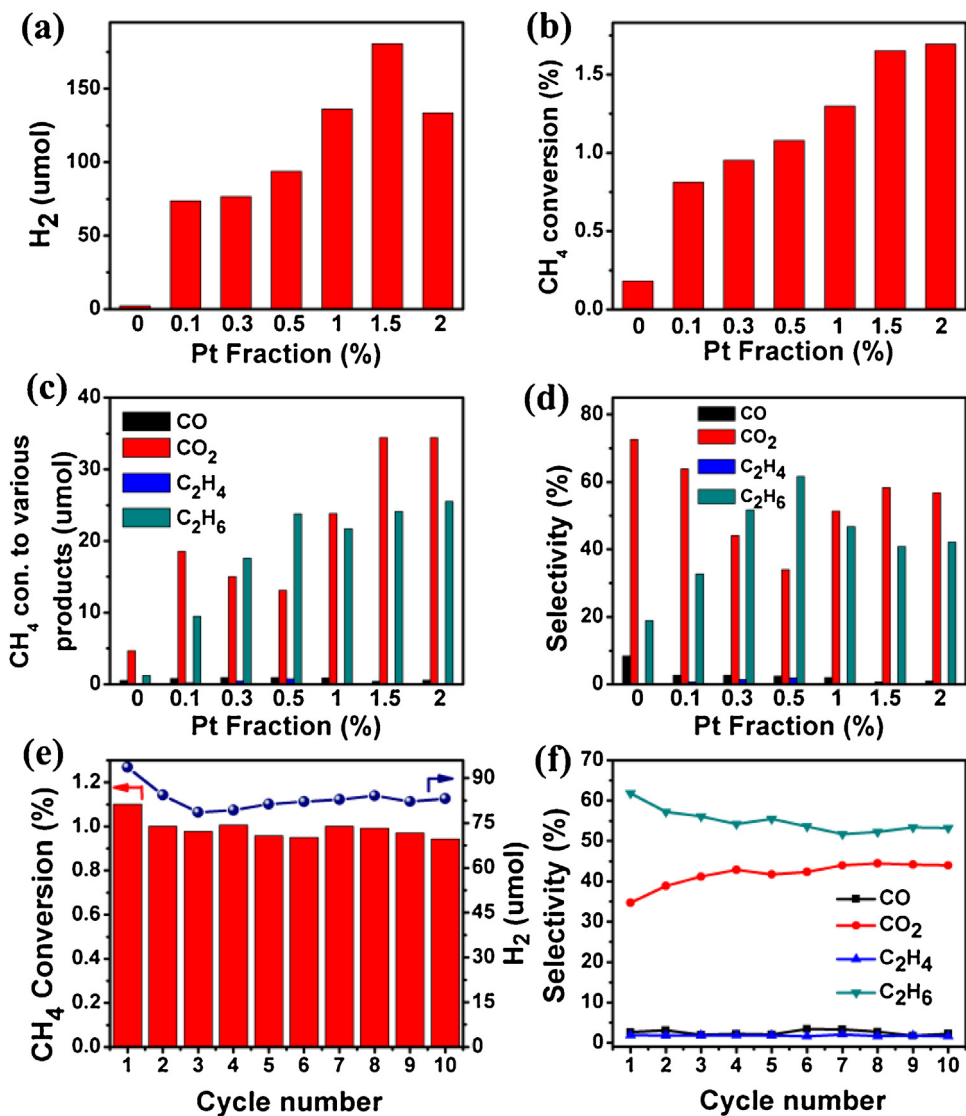


**Fig. 5.** The photocatalytic activities of (a) H<sub>2</sub> production, (b) CH<sub>4</sub> conversion, (c) CH<sub>4</sub> conversion to various carbonous gas products, (d) selectivity of carbonous products over x% Pt/TiO<sub>2</sub>, (e) stability of 0.5% Pt/TiO<sub>2</sub> in the recycling experiment and (f) selectivity of carbonous products over 0.5% Pt/TiO<sub>2</sub> in the recycling experiment. Reaction conditions: 80 mL pure CH<sub>4</sub>, 10 mL/min, 75 mg catalyst, 75 mL H<sub>2</sub>O, 6 h, ambient condition.

the selectivity of the production of C<sub>2</sub>H<sub>6</sub> and CO<sub>2</sub> (Fig. 5d), and 0.5% Pt/TiO<sub>2</sub> exhibits the highest selectivity for C<sub>2</sub>H<sub>6</sub> (61.7%). Considering the desired product of C<sub>2</sub>H<sub>6</sub>, we determine the 0.5% Pt/TiO<sub>2</sub> as the best photocatalyst. Furthermore, it exhibits the considerable stability in the recycling experiment in Fig. 5e. The H<sub>2</sub> production slightly decreases from 93.7 μmol for 1st run to 83.1 μmol for 10th run, and CH<sub>4</sub> conversion decreases from 1.1% for 1st run to 0.94% for 10th run. The selectivity for C<sub>2</sub>H<sub>6</sub> still maintains at 53.2% after ten cycles experiment (Fig. 5f).

### 3.3. Photocatalytic mechanism

The active species are crucial to the photocatalytic reaction, and their roles are examined by means of various scavengers. Ammonium oxalate is used as hole scavenger and Fe<sup>3+</sup> (Fe(NO<sub>3</sub>)<sub>3</sub> added) is used as electron scavenger under the similar reaction condition, and the results are shown in Fig. 6a–c. The trapping of hole dramatically decreases the conversion of CH<sub>4</sub> together with the decreasing of all the carbonous products seen in Fig. 6b and c. While the H<sub>2</sub> production increases from 93.7 μmol to 192.3 μmol in the presence of the trapping of holes (Fig. 6a), and it may be ascribed to the

increased electron availability. Similarly, the trapping of electron dramatically decreases the generation of H<sub>2</sub> (Fig. 6a). On the contrary, it increases the total conversion of CH<sub>4</sub> from 1.08% to 1.5% (Fig. 6b), which may be owed to the increased hole availability. Furthermore, the adding of the electron scavenger decreases the production of C<sub>2</sub>H<sub>6</sub> and increases the production of CO<sub>2</sub> simultaneously (Fig. 6c). It seems that the increased hole available tends to mineralize CH<sub>4</sub> into CO<sub>2</sub>. It is concluded from the results above that the photo-induced electron contributes to the generation of H<sub>2</sub> while hole is favourable to the conversion of CH<sub>4</sub>.

It is well known that Pt/TiO<sub>2</sub> possesses outstanding photocatalytically splitting of water into H<sub>2</sub> with the sacrificial agent for hole [40,50–52]. Is that possible that the participation of CH<sub>4</sub> facilitates the photocatalytic splitting of water into H<sub>2</sub> via consuming more hole? With Ar taking the place of CH<sub>4</sub>, the reaction is totally the photocatalytic water splitting. The compared results whether with CH<sub>4</sub> are presented in Fig. 6d (labelled H<sub>2</sub>O + CH<sub>4</sub> and H<sub>2</sub>O in the figure). It indicates that the introduction of CH<sub>4</sub> improves the H<sub>2</sub> production to almost 3 times. Without participation of H<sub>2</sub>O, only a little H<sub>2</sub> is obtained. And it experimentally proves the ability of CH<sub>4</sub> to produce H<sub>2</sub>. The results of Table S1 infer that the increasing amount

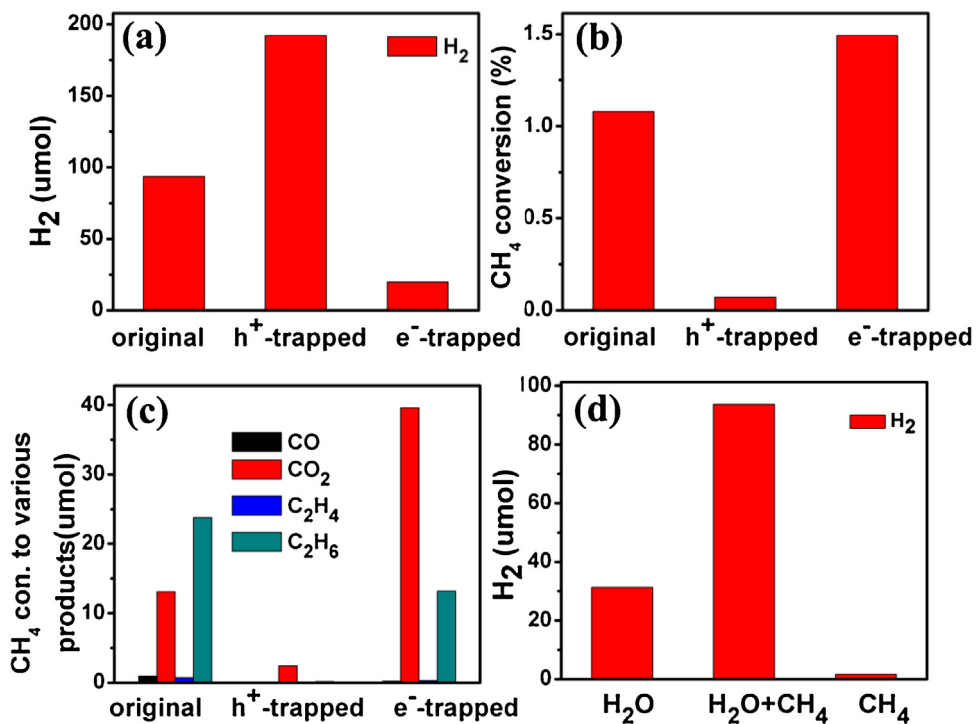


**Fig. 6.** The photocatalytic activities of (a)  $H_2$  production, (b)  $CH_4$  conversion and (c) carbonous gas product over 0.5% Pt/TiO<sub>2</sub> in various conditions. (d)  $H_2$  production over 0.5% Pt/TiO<sub>2</sub> with various reactants in the system.

of  $H_2$  is mainly derived from the water splitting after the participation of  $CH_4$ , while is lesser from  $CH_4$ . And it may put down to the improved separation of photo-induced hole and electron, through which way the participation of  $CH_4$  utilizes more holes and finally increases the electron availability. These results well provide the evidences of the synergistic effect for  $H_2$  evolution from water with  $CH_4$  conversion.

It is demonstrated above that the hole and electron play important roles for the yields of carbonous products and  $H_2$ . ESR spin-trapping technique with DMPO was conducted to confirm the roles of them or their derivative radicals. It is well known that an electron trapped by an  $O_2$  produces the  $\bullet O_2^-$ , and hereby the signal of  $\bullet O_2^-$  can be used to investigate the amount of electron. The results of Fig. 7a indicate that the introduction of Pt is prone to giving more  $\bullet O_2^-$ , in other words, Pt boosts the separation of photo-induced electrons and holes. Among them, 1.5% Pt/TiO<sub>2</sub> exhibits the strongest signal of  $\bullet O_2^-$ , which is experimentally proved to produce most  $H_2$ . It is therefore demonstrated that the electron takes part in the photocatalytic reaction to produce  $H_2$ . The  $\bullet OH$  is regarded as an oxidizing active species. The signal of  $\bullet OH$  gradually decreases along with the increase of the loading of Pt on TiO<sub>2</sub> (Fig. 7b). The  $\bullet CH_3$  presented in Fig. 7c is crucial combining to produce  $C_2H_6$ . We can learn that a little of Pt (0.1%) apparently raises the signal vested in  $\bullet CH_3$  [53–56], but more Pt gradually reduces the formation of  $\bullet CH_3$ . Moreover, the pure TiO<sub>2</sub> is able to produce the radical of  $\bullet CH_3$ , inferring that the  $CH_4$  molecular can be activated and dissociated on the TiO<sub>2</sub> particles. With a little Pt loaded on the surface of TiO<sub>2</sub>, the amount of  $\bullet CH_3$  remarkably increases. And it is deduced that the Pt on the surface of TiO<sub>2</sub> particle is favourable to the activation of  $CH_4$ . More Pt then reduces the formation of  $\bullet CH_3$ , as well as reduces the generation of  $\bullet OH$ , it is suggested that  $\bullet OH$  may be the key role for  $\bullet CH_3$  formation.

Moreover, the results of XPS indicate that the Pt loading on the surface of TiO<sub>2</sub> particles bonding with the oxygen of surface hydroxyl. And it is confirmed that the surface hydroxyl can be important mediator to generate hydroxyl radical [57,58]. With the

coverage of Pt at the site of surface hydroxyl, it is also verified that the amount of  $\bullet OH$  decreases in Fig. 7b, which further confirms the bonding of Pt with oxygen of surface hydroxyl.

It has been widely believed that the transition-metal could activate C–H in  $CH_4$  molecule [59], and it was confirmed that  $\bullet OH$  could be effective active species to dehydrogenate  $CH_4$  to form  $\bullet CH_3$  radical [26,27,48,60]. The mechanism should be proposed that with the activation of  $CH_4$  via Pt center, the C–H bond is weaken, and with the dehydrogenation of  $CH_4$  by  $\bullet OH$ , the  $\bullet CH_3$  then forms. Based on that Pt loading may reduce the generation of  $\bullet OH$ . The increasing of Pt loading may improve the activation of  $CH_4$ , but also reduces the amount of  $\bullet OH$  since Pt coverage of surface hydroxyl may inhibit the dehydrogenation. Hence the proper Pt loading results in the efficient cooperation between the activation of  $CH_4$  over Pt site and dehydrogenation of  $CH_4$  by  $\bullet OH$ , which may be a clue factor for the reaction.

The quantum efficiency (QE) is an important indicator in the determination of photocatalytic reaction. The QE for  $H_2$  production is calculated as 4.7%, which is higher than 2% of which Pt/TiO<sub>2</sub> reacting  $CH_4$  gas with  $H_2O$  vapour [61]. The QE for  $CH_4$  conversion is calculated as 3.3% (calculation details seen in the Supporting information).

Thus far, direct combination of the photocatalytic coupling of  $CH_4$  and the synergistic reaction of  $H_2$  evolution from water was studied. It is demonstrated that the introduction of Pt may activate the C–H bond of  $CH_4$  to form more  $\bullet CH_3$ , which was consist with the results of C–H activation at the transition-metal centres [59]. The subsequent coupling of  $\bullet CH_3$  brings up the product of  $C_2H_6$ , and the coupling of  $\bullet CH_2$  which is formed by further dehydrogenated from  $\bullet CH_3$  leads to the generation of  $C_2H_4$ . Based on the fact that a little  $C_2H_4$  and no  $C_2H_2$  formed in the reaction system, it is considered difficult to further generate  $\bullet CH_2$  from  $\bullet CH_3$  and hardly possible to yield  $\bullet CH$  from  $\bullet CH_2$ . Thereby the generation of  $CO_2$  is attributed to the oxidation of  $CH_4$  or  $\bullet CH_3$  by hole or molecule oxygen (generated from water splitting). Focusing on the performance of photo-generated electron, it will react with  $H^+$  to

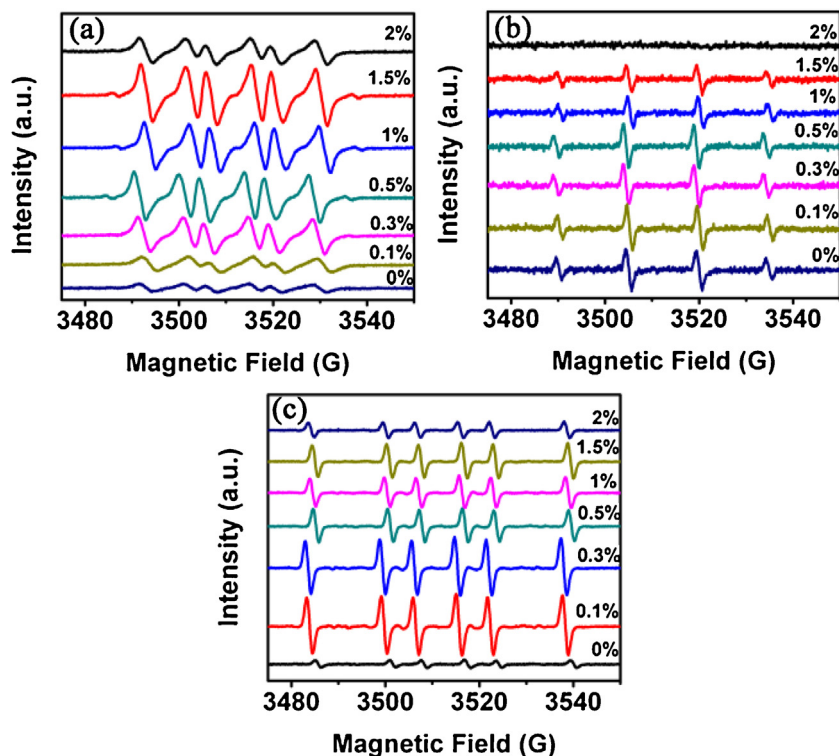
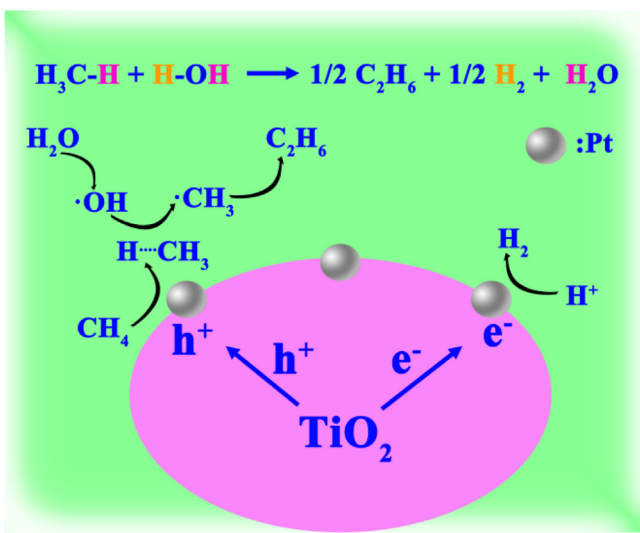
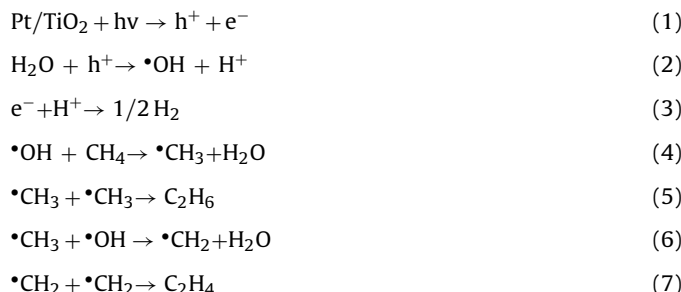


**Fig. 7.** ESR spectra of  $O_2\bullet^-$  (a),  $\cdot OH$  (b) and  $\cdot CH_3$  (c) radical species trapped by DMPO over Pt/TiO<sub>2</sub> series dispersions.



**Scheme 1.** The proposed mechanism of the photocatalytic process.

gives rise to the generation of H<sub>2</sub>. The photocatalytic mechanism is proposed in [Scheme 1](#), and the processes are hypothesized as follow:



#### **4. Conclusions**

In summary, we describe a new synergistic photocatalytic system in which the coupling of CH<sub>4</sub> to high-valued products plays an important role in enhancing the photocatalytic splitting of water into H<sub>2</sub>. The Pt loading on TiO<sub>2</sub> is an efficient way to improve the yields of both H<sub>2</sub> and C<sub>2</sub>H<sub>6</sub> products. The synergistic effect between the two involved reactions gives more efficient separation and adequate utilization of photo-induced electron and hole, and the photo-induced electron contributes to the generation of H<sub>2</sub> while hole is favourable to the conversion of CH<sub>4</sub>. The proper Pt loading results in the efficient cooperation between the activation of CH<sub>4</sub> over Pt site and dehydrogenation of CH<sub>4</sub> by •OH, afterward appropriate amount of •CH<sub>3</sub> is produced, and then C<sub>2</sub>H<sub>6</sub> is formed. The new strategy of the photocatalytic reaction realizes synergistically selective coupling of CH<sub>4</sub> and H<sub>2</sub> production from aqueous water, and improves the efficiency in photocatalysis (with QE of 4.7% for H<sub>2</sub> generation and 3.3% for CH<sub>4</sub> conversion). We believe that the bridged photocatalytic pathway can provide some valuable information for extending water-gas reactions in future.

### **Acknowledgment**

This work was financially supported by the National Natural Science Foundation (NNSF) of China (21173047 and 21373049).

## Appendix A. Supplementary data

Supplementary data associated with this article can be found, in the online version, at <http://dx.doi.org/10.1016/j.apcatb.2016.11.039>.

## References

- [1] R. Broun, M. Sattler, A comparison of greenhouse gas emissions and potential electricity recovery from conventional and bioreactor landfills, *J. Clean. Prod.* 112 (Part 4) (2016) 2664–2673.
- [2] R. de.Richter, S. Caillol, Fighting global warming: the potential of photocatalysis against CO<sub>2</sub> CH<sub>4</sub>, N<sub>2</sub>O, CFCs, tropospheric O<sub>3</sub>, BC and other major contributors to climate change, *J. Photochem. Photobiol. C: Photochem. Rev.* 12 (2011) 1–19.
- [3] S.A.M. Said, M. Waseeuddin, D.S.A. Simakov, A review on solar reforming systems, *Renew. Sustain. Energy Rev.* 59 (2016) 149–159.
- [4] D. Pakhare, J. Spivey, A review of dry (CO<sub>2</sub>) reforming of methane over noble metal catalysts, *Chem. Soc. Rev.* 43 (2014) 7813–7837.
- [5] X.-S. Li, A.-M. Zhu, K.-J. Wang, Y. Xu, Z.-M. Song, Methane conversion to C<sub>2</sub> hydrocarbons and hydrogen in atmospheric non-thermal plasmas generated by different electric discharge techniques, *Catal. Today* 98 (2004) 617–624.
- [6] V. Lomonosov, Y. Gordienko, M. Sinev, Effect of water on methane and ethane oxidation in the conditions of oxidative coupling of methane over model catalysts, *Top. Catal.* 56 (2013) 1858–1866.
- [7] D. Papageorgiou, A.M. Efstratiou, X.E. Verykios, The selective oxidation of methane to C<sub>2</sub>-hydrocarbons over lithium-doped TiO<sub>2</sub> catalysts, *Appl. Catal. A: Gen.* 111 (1994) 41–62.
- [8] T.H. Pham, Y. Qi, J. Yang, X. Duan, G. Qian, X. Zhou, D. Chen, W. Yuan, Insights into Hägg iron-carbide-catalyzed Fischer-Tropsch synthesis: suppression of CH<sub>4</sub>Formation and enhancement of CC coupling on  $\chi$ -Fe5C2(510), *ACS Catal.* 5 (2015) 2203–2208.
- [9] P.E. Savage, R. Li, J.T. Santini, Methane to methanol in supercritical water, *J. Supercrit. Fluids* 7 (1994) 135–144.
- [10] Y. Teng, H. Sakurai, K. Tabata, E. Suzuki, Methanol formation from methane partial oxidation in CH<sub>4</sub>–O<sub>2</sub>–NO gaseous phase at atmospheric pressure, *Appl. Catal. A: Gen.* 190 (2000) 283–289.
- [11] A. Indarto, A review of direct methane conversion to methanol by dielectric barrier discharge, *ITDEI* 15 (2008) 1038–1043.
- [12] J.S. Han, C.M. Ahn, B. Mahanty, C.G. Kim, Partial oxidative conversion of methane to methanol through selective inhibition of methanol dehydrogenase in methanotrophic consortium from landfill cover soil, *Appl. Biochem. Biotechnol.* 171 (2013) 1487–1499.
- [13] X. Guo, G. Fang, G. Li, H. Ma, H. Fan, L. Yu, C. Ma, X. Wu, D. Deng, M. Wei, D. Tan, R. Si, S. Zhang, J. Li, L. Sun, Z. Tang, X. Pan, X. Bao, Direct, nonoxidative conversion of methane to ethylene, aromatics, and hydrogen, *Sci* 344 (2014) 616–619.
- [14] J.J. Spivey, G. Hutchings, Catalytic aromatization of methane, *Chem. Soc. Rev.* 43 (2014) 792–803.
- [15] N.S. Lewis, D.G. Nocera, Powering the planet: chemical challenges in solar energy utilization, *Proc. Natl. Acad. Sci. U. S. A.* 103 (2006) 15729–15735.
- [16] Y. Kato, H. Yoshida, T. Hattori, Photoinduced non-oxidative coupling of methane over silica-alumina and alumina around room temperature, *Chem. Commun.* (1998) 2389–2390.
- [17] A.R. Derk, H.H. Funke, J.L. Falconer, Methane conversion to higher hydrocarbons by UV irradiation, *Ind. Eng. Chem. Res.* 47 (2008) 6568–6572.
- [18] L. Yuliati, T. Hattori, H. Itoh, H. Yoshida, Photocatalytic nonoxidative coupling of methane on gallium oxide and silica-supported gallium oxide, *J. Catal.* 257 (2008) 396–402.
- [19] K. Shimura, T. Yoshida, H. Yoshida, Photocatalytic activation of water and methane over modified gallium oxide for hydrogen production, *J. Phys. Chem. C* 114 (2010) 11466–11474.
- [20] A. Hameed, M.A. Gondal, Production of hydrogen-rich syngas using p-type NiO catalyst: a laser-based photocatalytic approach, *J. Mol. Catal. A: Chem.* 233 (2005) 35–41.
- [21] K. Shimura, H. Yoshida, Semiconductor photocatalysts for non-oxidative coupling, dry reforming and steam reforming of methane, *Catal. Surv. Asia* 18 (2014) 24–33.
- [22] K. Shimura, H. Kawai, T. Yoshida, H. Yoshida, Bifunctional rhodium cocatalysts for photocatalytic steam reforming of methane over alkaline titanate, *ACS Catal.* 2 (2012) 2126–2134.
- [23] H. Liu, X. Meng, T.D. Dao, H. Zhang, P. Li, K. Chang, T. Wang, M. Li, T. Nagao, J. Ye, Conversion of carbon dioxide by methane reforming under visible-light irradiation: surface-plasmon-mediated nonpolar molecule activation, *Angew. Chem. Int. Ed. Engl.* 54 (2015) 11545–11549.
- [24] M.A. Gondal, A. Hameed, A. Suwaiyan, Photo-catalytic conversion of methane into methanol using visible laser, *Appl. Catal. A: Gen.* 243 (2003) 165–174.
- [25] C.E. Taylor, R.P. Noceti, New developments in the photocatalytic conversion of methane to methanol, *Catal. Today* 55 (2000) 259–267.
- [26] R.P. Noceti, C.E. Taylor, J.R. D'Este, Photocatalytic conversion of methane, *Catal. Today* 33 (1997) 199–204.
- [27] C.E. Taylor, Methane conversion via photocatalytic reactions, *Catal. Today* 84 (2003) 9–15.
- [28] A. Hameed, I.M.I. Ismail, M. Aslam, M.A. Gondal, Photocatalytic conversion of methane into methanol: performance of silver impregnated WO<sub>3</sub>, *Appl. Catal. A: Gen.* 470 (2014) 327–335.
- [29] S. Murcia-López, K. Villa, T. Andreu, J.R. Morante, Partial oxidation of methane to methanol using bismuth-based photocatalysts, *ACS Catal.* 4 (2014) 3013–3019.
- [30] K. Villa, S. Murcia-López, T. Andreu, J.R. Morante, Mesoporous WO<sub>3</sub> photocatalyst for the partial oxidation of methane to methanol using electron scavengers, *Appl. Catal. B: Environ.* 163 (2015) 150–155.
- [31] L. Li, S. Fan, X. Mu, Z. Mi, C.J. Li, Photoinduced conversion of methane into benzene over GaN nanowires, *J. Am. Chem. Soc.* (2014).
- [32] Y. Yu, T. He, L. Guo, Y. Yang, L. Guo, Y. Tang, Y. Cao, Efficient visible-light photocatalytic degradation system assisted by conventional Pd catalysis, *Sci. Rep.* 5 (2015) 9561.
- [33] L. Xu, J. Liu, Y. Hong, Y. Xu, Q. Wang, L. Lin, Regeneration behaviors of Fe/Si-2 and Fe-Mn/Si-2 catalysts for C<sub>x</sub>H<sub>y</sub>(6) dehydrogenation with CO<sub>2</sub> to C<sub>x</sub>H<sub>y</sub>(4), *Catal. Lett.* 62 (1999) 185–189.
- [34] M. Huff, L.D. Schmidt, Ethylene formation by oxidative dehydrogenation of ethane over monoliths at very short contact times, *J. Phys. Chem.* 97 (1993).
- [35] S.A. Kandel, T.P. Rakitzis, T. Lev-On, R.N. Zare, Dynamics for the Cl + C<sub>2</sub>H<sub>6</sub> → HCl + C<sub>2</sub>H<sub>5</sub> reaction examined through state-specific angular distributions, *J. Chem. Phys.* 105 (1996) 7550–7559.
- [36] R.T. Carroll, E.D.J. Witt, L.E. Trapasso, Oxychlorination of lower alkanes, US, 1965.
- [37] J.A. Cowfer, V.J. Johnston, L. Popiel, Method for reducing formation of polychlorinated aromatic compounds during air oxychlorination of C 1–C 3 Hydrocarbons, EP (1997).
- [38] L.J. Croce, L. Bajars, M. Gablik, Oxychlorination of hydrocarbons in the presence of non-halide copper containing catalysts, 1977.
- [39] A. HAGEN, F. ROESSNER, Ethane to aromatic hydrocarbons: past, present, Future CarRv 42 (2000) 403–437.
- [40] A. Kudo, Y. Miseki, Heterogeneous photocatalyst materials for water splitting, *Chem. Soc. Rev.* 38 (2009) 253–278.
- [41] X. Wang, K. Maeda, A. Thomas, K. Takanabe, G. Xin, J.M. Carlsson, K. Domen, M. Antonietti, A metal-free polymeric photocatalyst for hydrogen production from water under visible light, *Nat. Mater.* 8 (2009) 76–80.
- [42] X. Chen, L. Liu, P.Y. Yu, S.S. Mao, Increasing solar absorption for photocatalysis with black hydrogenated titanium dioxide nanocrystals, *Sci* 331 (2011) 746–750.
- [43] T.S. Teets, D.G. Nocera, Photocatalytic hydrogen production, *Chem. Commun. (Camb.)* 47 (2011) 9268–9274.
- [44] A. Tiwari, U. Pal, Effect of donor-donor-π-acceptor architecture of triphenylamine-based organic sensitizers over TiO<sub>2</sub> photocatalysts for visible-light-driven hydrogen production, *Int. J. Hydrogen Energy* 40 (2015) 9069–9079.
- [45] B. Erdem, R.A. Hunicker, G.W. Simmons, E.D. Sudol, V.L. Dimonie, M.S. El-Aasser, XPS and FTIR surface characterization of TiO<sub>2</sub> particles used in polymer encapsulation, *Langmuir* 17 (2001) 2664–2669.
- [46] B. Xin, L. Jing, Z. Ren, B. Wang, H. Fu, Effects of simultaneously doped and deposited Ag on the photocatalytic activity and surface states of TiO<sub>2</sub>, *J. Phys. Chem. B* 109 (2005) 2805–2809.
- [47] K. Villa, S. Murcia-López, J.R. Morante, T. Andreu, An insight on the role of La in mesoporous WO<sub>3</sub> for the photocatalytic conversion of methane into methanol, *Appl. Catal. B: Environ.* 187 (2016) 30–36.
- [48] K. Ogura, M. Kataoka, Photochemical conversion of methane, *J. Mol. Catal.* 43 (1988) 371–379.
- [49] M.A. Gondal, A. Hameed, Z.H. Yamani, A. Arfaj, Photocatalytic transformation of methane into methanol under UV laser irradiation over WO<sub>3</sub>, TiO<sub>2</sub> and NiO catalysts, *Chem. Phys. Lett.* 392 (2004) 372–377.
- [50] C.R. López, E.P. Melián, J.A. Ortega Méndez, D.E. Santiago, J.M. Doña Rodríguez, O. González Díaz, Comparative study of alcohols as sacrificial agents in H<sub>2</sub> production by heterogeneous photocatalysis using Pt/TiO<sub>2</sub> catalysts, *J. Photochem. Photobiol. A: Chem.* 312 (2015) 45–54.
- [51] A. Patsoura, D.I. Kondarides, X.E. Verykios, Enhancement of photoinduced hydrogen production from irradiated Pt/TiO<sub>2</sub> suspensions with simultaneous degradation of azo-dyes, *Appl. Catal. B: Environ.* 64 (2006) 171–179.
- [52] J. Yu, L. Qi, M. Jaroniec, Hydrogen production by photocatalytic water splitting over Pt/TiO<sub>2</sub>Nanosheets with exposed (001) facets, *J. Phys. Chem. C* 114 (2010) 13118–13125.
- [53] I. Ueno, M. Hoshino, T. Maitani, S. Kanegasaki, Y. Ueno, Luteoskyrin, an anthraquinoid hepatotoxin and ascorbic-acid generate hydroxyl radical in-vitro in the presence of a trace amount of ferrous iron, *Free Radic. Res. Commun.* 19 (1993) S95–S100.
- [54] H. Taniguchi, K.P. Madden, DMPO-Alkyl radical spin trapping: an In Situ Radiolysis steady-state ESR study, *Radiat. Res.* 153 (2000) 447–453.
- [55] R. Dabestani, R.D. Hall, R.H. Sik, C.F. Chignell, Spectroscopic studies of cutaneous photosensitizing agents—XV. Anthralin and its oxidation product 1,8-dihydroxyanthraquinone, *Photochem. Photobiol.* 52 (1990) 961–971.
- [56] C.M. Jones, M.J. Burkitt, EPR spin-trapping evidence for the direct, one-electron reduction of tert-butylhydroperoxide to the tert-butoxyl radical by copper(II): paradigm for a previously overlooked reaction in the initiation of lipid peroxidation, *J. Am. Chem. Soc.* 125 (2003) 6946–6954.
- [57] M.A. Henderson, Structural sensitivity in the dissociation of water on TiO<sub>2</sub> single-crystal surfaces, *Langmuir* 12 (1996) 5093–5098.

[58] P. Jones, J.A. Hockey, Infrared studies of rutile surfaces. Part 3.7 Adsorption of water and dehydroxylation of rutile, *J. Chem. Soc. Faraday Trans.* 68 (1972) 907–913.

[59] J.A. Labinger, J.E. Bercaw, Understanding and exploiting CH bond activation, *Nature* 417 (2002) 507–514.

[60] K. Villa, S. Murcia-López, T. Andreu, J.R. Morante, On the role of WO<sub>3</sub> surface hydroxyl groups for the photocatalytic partial oxidation of methane to methanol, *Catal. Commun.* 58 (2015) 200–203.

[61] H. Yoshida, K. Hirao, J.-i. Nishimoto, K. Shimura, S. Kato, H. Itoh, T. Hattori, Hydrogen production from methane and water on platinum loaded titanium oxide photocatalysts, *J. Phys. Chem. C* 112 (2008) 5542–5551.